Indian Journal of Pure & Applied Physics
Vol. 62, July 2024, pp. 562-569
DOI: 10.56042/ijpap.v62i7.8435

Olive Oil Lampblack for Supercapacitor Electrodes

Prakash Joshi[a*], Umesh Lawaju[b], Mim Lal Nakarmi[c], Ram Chandra Rai[d], Sabina Khatri[e] & Ramani Pradhan[f]

[a]Physics Department, Bhaktapur Multiple Campus, Tribhuvan University, Bhaktapur 44800, Nepal

[b]Department of Physics, Patan Multiple Campus, Tribhuvan University, Lalitpur 44800, Nepal

[c]Department of Physics, Brooklyn College and the Graduate Center of the City University of New York, Brooklyn, NY 11210, USA

[d]Department of Physics, SUNY Buffalo State, Buffalo, NY 14222, USA

[e]Central Department of Chemistry, Tribhuvan University, Kritipur 44800, Nepal

[f]Department of Applied Sciences and Chemical Engineering, Pulchowk Campus, Institute of Engineering, Tribhuvan University, Lalitpur 44800, Nepal

Received 31 January 2024; accepted 17 May 2024

In this study, we prepared and characterized lampblack of olive oil for application in supercapacitors. The lampblack was prepared by the simple technique of flame-soot method. The lampblack samples characterized by using X-ray Diffraction (XRD), Raman spectroscopy, Fourier Transform Infrared Spectroscopy (FTIR), N_2 adsorption-desorption isotherms, Scanning Electron Microscopy (SEM), and Energy Dispersive X-ray Spectroscopy (EDS) revealed that they contain mostly amorphous nanosized carbon particles with oxygenated functional groups and the carbon content in the lampblack was 92.6%. The surface area of the lampblack carbon calculated from the Brunauer-Emmett-Teller (BET) method was found to be about 302.7 m^2g^{-1} with an average pore size of 1.69 nm obtained from the Density Functional Theory (DFT) analysis. Lampblack carbon samples were used to prepare supercapacitor electrodes. Electrochemical properties of the electrodes were investigated in 6M aqueous KOH by Cyclic Voltammetry (CV), Galvanostatic Charge Discharge (GCD), and Electrochemical Impedance Spectroscopy (EIS) techniques. The specific capacitance of the electrode obtained from the GCD test was 70.36 Fg^{-1} at the current density of 1 Ag^{-1} with a low Equivalent Series Resistance (ESR) value of 0.81 Ω.

Keywords: Lampblack; Supercapacitor; Hierarchical pores; Flame-soot method

1 Introduction

Concept of high capacitance device, super capacitorusing fired tar lampblack as an electrode material was proposed by Becker in 1957[1–3]. The supercapacitor using the lampblack was capable of obtaining a high capacitance of up to 6 F at 1.5 V. The electrode material was porous carbonaceous material immersed in a liquid electrolyte. Charge storage mechanism in such supercapacitor is based on the principle of double-layer capacitance and the supercapacitors are called electrochemical double-layer capacitors (EDLCs). Electrical energy in the EDLC is stored electrostatically at the interface of the electrode and the electrolyte. So, there is no transfer of charge between the electrode and the electrolyte[3]. Therefore, the supercapacitor based on double-layer capacitance possesses extremely long cyclic life and fast charge-discharge rates. Another type of energy storage mechanism is pseudocapacitance in which energy is stored by the transfer of charge between electrode and electrolyte through chemisorption, reduction-oxidation reactions, and intercalation process[2]. Since chemical reactions are not entirely reversible, pseudocapacitors have low cyclic life and delayed response compared to EDLCs[2,4].

Despite having long charge-discharge life, high power density, and low equivalent series resistance (ESR), the major disadvantage of supercapacitors is their low energy density. The energy density of a supercapacitor is given by $\frac{1}{2}CV^{22}$. From this relation, energy density can be improved either by increasing the specific capacitance or increasing the operating voltage. For an aqueous electrolyte, the operating voltage is limited to 1.2V[5]. For a non-aqueous electrolyte such as organic and ionic liquids, the operating voltage can be boosted up to 3.0V and 4.0V, respectively[5]. However, the low conductivity and stability issue of organic electrolytes in air and the higher viscous nature of ionic liquid that prevents the smooth transfer of ions are a setback in using non-aqueous electrolytes[3]. So, aqueous electrolyte is used for practical and safety reasons. Many researchers are, therefore, focusing on improving the

*Corresponding author:
(E-mail: prakash.joshi@bkmc.tu.edu.np)

specific capacitance of the electrode which depends on the surface textural properties of the materials used on the electrodes.

In EDLCs, carbon materials of different surface textures have been explored such as activated carbon[6–9], carbon nanotubes[10], carbon nanofibers[11], graphene[12], and mesoporous carbon microspheres[13]. Among them, activated carbons are widely used as electrode material since these materials provide excellent surface area but they may suffer from low conductivity. So, during the preparation of the electrode using activated carbon, carbon black is added to improve its electric conductivity[12]. Some researchers have used carbon black or its type such as lampblack, as the active material of supercapacitor electrodes and reported promising results[12,14–18]. Lampblack is a carbonaceous material produced as soot due to the incomplete combustion of oil or other combustible organic materials. Previously, we used lampblack of mustard oil and soybean oil to prepare an electrode of the Dye-sensitized solar cells (DSCs) and reported its excellent catalytic performance[19,20]. Similarly, we have employed soybean oil based lampblack as a sole electrode material (without any additional conductive material) of EDLC and obtained specific capacitance of 49.27 Fg^{-1} at 1 Ag^{-1}[21]. Singh *et al.* used diesel soot obtained from the exhaust of a vehicle as the supercapacitor electrode material and reported a specific capacitance of 36.77 Fg^{-1}[14]. In this research, we have explored lampblack of olive oil as a sole electrode material for the application in supercapacitor electrode. Using the lampblack of olive oil as a novel supercapacitor electrode material, we obtained a capacitance of 70.36 Fg^{-1} at 1 Ag^{-1} with a low ESR of 0.81Ω.

2 Experimental

2.1 Preparation of Olive oil Lampblack Samples and Characterization

Lampblack of olive oil was prepared using the similar flame-soot method described by Joshi *et. al.*[19,22]. The flame of olive oil was covered with the concave surface of a cleaned mortar. Lampblack (soot) was then deposited on the concave surface. The prepared lampblack samples were collected and characterized. As the capacitive performance of the electrodes of a supercapacitor depends on the surface morphology and surface texture such as porosity, specific surface area, shape, and size of the materials used in the electrodes[13,23–25],the lampblack was characterized to study those physical properties using different characterization techniques. Surface morphology and elemental composition of the sample were explored with Scanning Electron Microscopy (SEM) and Energy Dispersive X-ray Spectroscopy (EDS), respectively by using FEI Helios Nanolab 660 Scanning electron microscope, Thermo Fisher Scientific, USA. X-Ray Diffraction (XRD) was used to study the structure of the material. The XRD was carried out by using Rigaku MiniFlex 600 diffractometer with the Cu Kα source (λ = 1.54 Å). Raman spectroscopy was used to determine composition of ordered and disordered carbon phases in the sample. The surface area and porosity of the sample were investigated using Autosorb-1C (Quantachrome, USA) Brunauer-Emmett-Teller (BET) surface area and porosity analyzer. Fourier Transform Infrared Spectroscopy (FTIR) of the sample was carried out to determine functional groups by using IRTracer-100 (Shimadzu).

2.2 Preparation of Lampblack-Based Capacitors for Electrochemical Measurements

The electrochemical characterization was performed by three electrodes system where lampblack carbon electrodes were used as working electrode, platinum wire as counter electrode, and Ag/AgCl electrode as reference electrode. 6 M aqueous KOH solution was used as electrolyte. For the preparation of working electrode, a mixture of 4 mg of olive oil lampblack powder and 0.5 mg of polyvinylidene fluoride (PVDF) (from Apollo Scientific) were ground in a mortar. Then about 100 µL of 1-Methyl-2-pyrrolidinone (from Glentham Life Sciences) was added to disperse PVDF. The obtained mixed slurry was then coated on a nickel foam of size 1 cm^2. Then, it was dried at ~70 ºC overnight. Here PVDF was used as binder only. The dried electrodes were then pressed and soaked overnight in 6 M aqueous KOH solution before the electrochemical measurement.

Electrochemical measurements were performed using Interface 1010E (Gamry Instrument, USA) and the capacitive performances were evaluated by cyclic voltammetry (CV) and galvanostatic charge–discharge tests (GCD).The Electrochemical Impedance Spectroscopy (EIS) of the electrode was performed in potentiostatic mode with 10 mV AC signals of frequencies ranging from 0.1 Hz to 100 KHz.

3 Results and discussion

3.1 Characterization results

Figure 1 shows the XRD pattern of the olive oil lampblack sample. The XRD pattern revealed two broad characteristics peaks of carbon centered around

24.7° and 43.5° corresponding to the reflection from (002) and (100) planes, respectively[26]. This indicates that lampblack consists of graphitic carbon and dominant amorphous carbon[27,28].

Figure 2 is the Raman spectrum of the olive oil lampblack and it shows two typical absorption bands of carbon at 1340 cm^{-1} and 1591 cm^{-1}, attributed to D-band and G-band, respectively[14,24,27]. The Raman spectrum is fitted using Lorentzian line shapes with background subtraction to calculate the portion of disordered and ordered carbon in the sample [29]. The intensity ratio of D and G bands, I_D/I_G calculated by integrating the area under the corresponding peak is found to be 1.48. This means higher content of amorphous carbon compared to the crystalline carbon in the sample [24]. This result is consistent with the result from XRD shown in the Fig. 1.

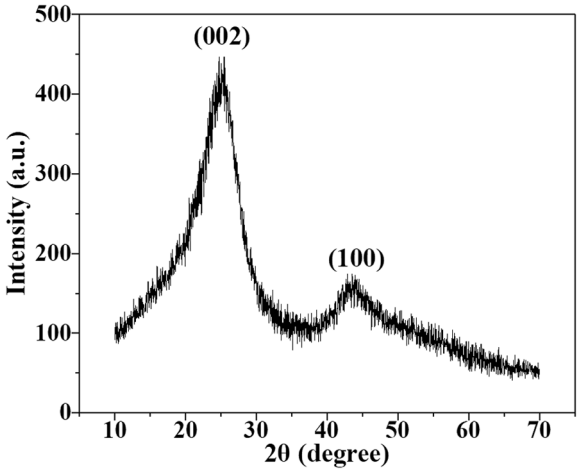

Fig. 1 — XRD pattern of lampblack sample of olive oil

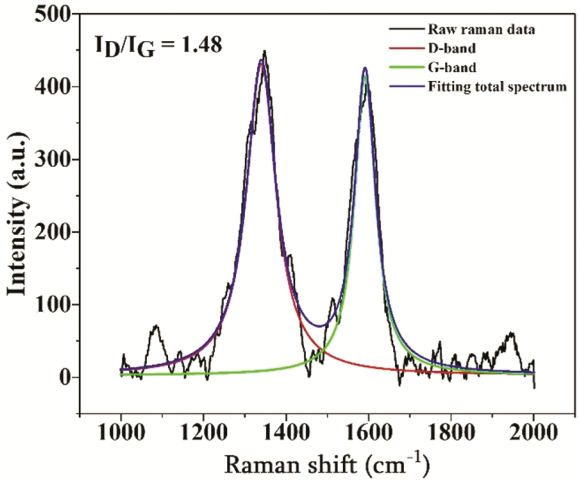

Fig.2 — Raman spectrum of lampblack sample of olive oil

Figure 3 shows the SEM images of lampblack sample at different magnifications. The SEM images show that the carbon particles are closely packed agglomerates of smaller primary particles of size about 100 nm. This result is in alignment with the soot produced from diesel and candle[14,16]. Also, the carbon particles form an interconnected structures which may enhance the conductivity of the electrode.

The EDS spectrum shown in Fig. 4 revealed high concentration of carbon (92.6%). It also contains a small concentration of oxygen (4.5%) and other elements (2.9%). The presence of oxygen may be due to the remnants of different oxygen function groups and the absorbed water vapour from the air in the sample. The presence of small amount of chlorine, zinc, and sodium could be due to the contamination of the sample.

For the detection of functional groups present in the lampblack, FTIR was carried out. Fig. 5 shows the FTIR spectra of lampblack after background correction. The broad adsorption band around 3445 cm^{-1} corresponds to O-H stretching, which implies the existence of absorbed water vapor in the sample[26,27]. The strong and sharp peak at around 2345 cm^{-1} is due to CO_2[26]. The peak at around 1595 cm^{-1} can be associated to the stretching of carboxylic acid[26]. Similarly, the peak at around 1230 cm^{-1} can be associated to C-O stretching of alkyl aryl ether[30].

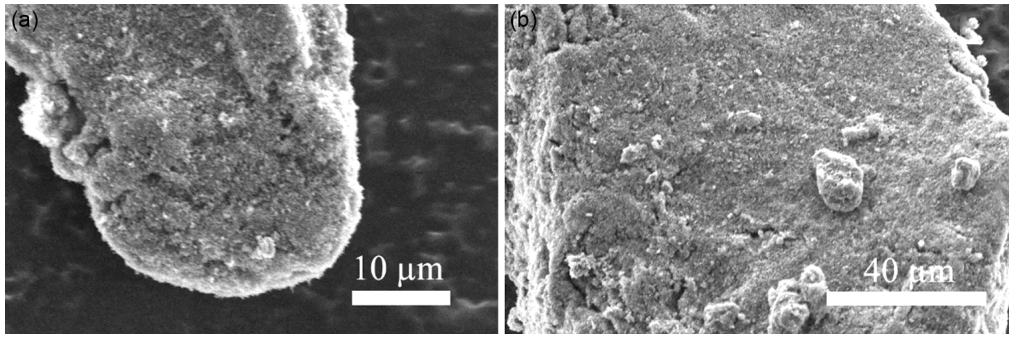

Fig 3 — SEM image (a) at ~2500 x magnification and (b) ~1000 x magnification

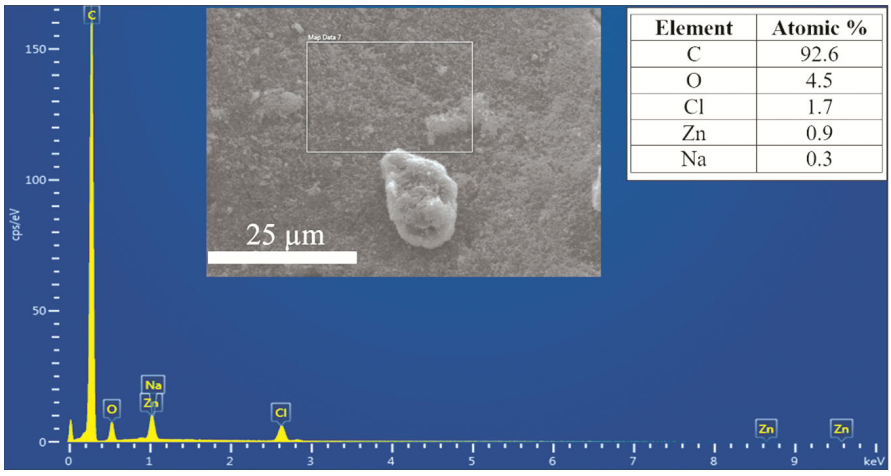

Element	Atomic %
C	92.6
O	4.5
Cl	1.7
Zn	0.9
Na	0.3

Fig. 4 — EDS spectrum of lampblack sample. The SEM image is displayed in the inset, and the EDS scanned area is indicated by a rectangle

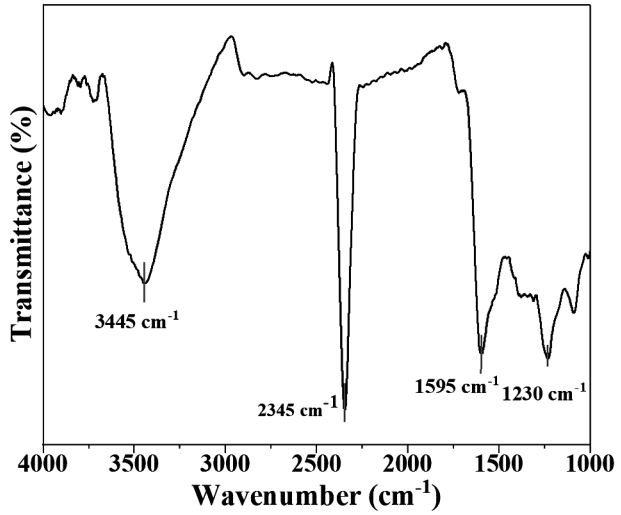

Fig. 5 — FTIR spectrum of lampblack

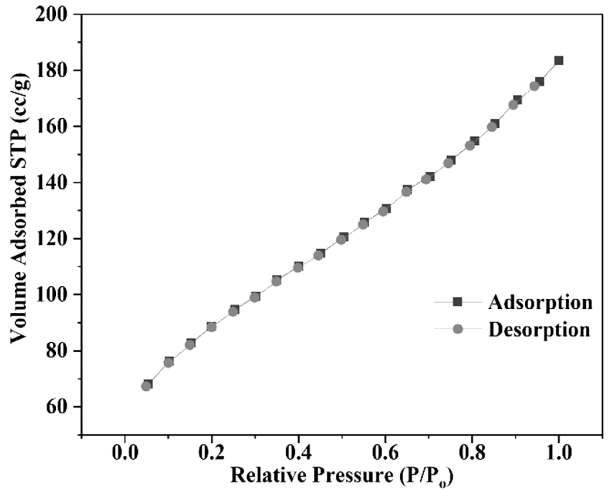

Fig. 6 — Nitrogen adsorption-desorption isotherm.

Capacitive performance of a supercapacitor electrode depends on the textural properties of the electrode material. So, N_2 adsorption-desorption isotherms were obtained and surface area, pore volume and pore size of the sample were determined. These parameters are tabulated in Table 1. The ratio of micropore area to the specific surface area is 59.8%, which indicates slightly higher concentration of micropores in the sample.

Figure 6 shows the N_2 adsorption-desorption isotherm curve. The isotherm shows the volume of the gas adsorption increased almost linearly with the relative pressure indicating multilayered gas adsorption. Thus, the isotherm roughly corresponds to type II isotherm[31]. Total pore volume (the cumulative pore volume of micropores, mesopores, and macropores calculated from Multipoint BET) was 0.2844 ccg^{-1}. The surface area of the lampblack carbon of olive oil is 302.7 m^2g^{-1} which is greater than the soot of diesel[14] and candle[17]. Also, the pore size distributions obtained from Barrett–Joyner–Halenda (BJH) method, Fig. 7(a), and density functional theory (DFT) method, Fig 7(b) indicate the presence of micropores (< 2 nm) and mesopores (2- 50 nm). The estimated pore size for most of the pores were 1.6879 nm and 1.937 nm from DFT and BJH methods, respectively. The tails in the distributions show existence of higher pore size up to mesopores. This suggests that the pore structure of olive oil lampblack was hierarchal in nature. The availability of micropores ensures the high surface area for the formation of double layer and hence higher capacitance, whereas mesopores provide the pathway for the smooth transfer of ions into the deeper part of the electrode[5,32].

Table 1 — Specific surface area and pore characteristics of lampblack carbon

$S_{BET}(m^2g^{-1})$	S_{micro} (m^2g^{-1})	S_{micro}/S_{BET}	W_{DFT} (nm)	$V_{DFT}(ccg^{-1})$	$V_{micro}(ccg^{-1})$	$V_{meso}(ccg^{-1})$
302.7	181.1	59.8%	1.6879	0.2563	0.09705	0.1593

S_{BET} = specific surface area, S_{micro} = micropore area, W_{DFT} = pore width (mode) using DFT method, V_{DFT} = volume using DFT analysis, V_{micro} = micropore volume, and $V_{meso} = V_{DFT} - V_{micro}$

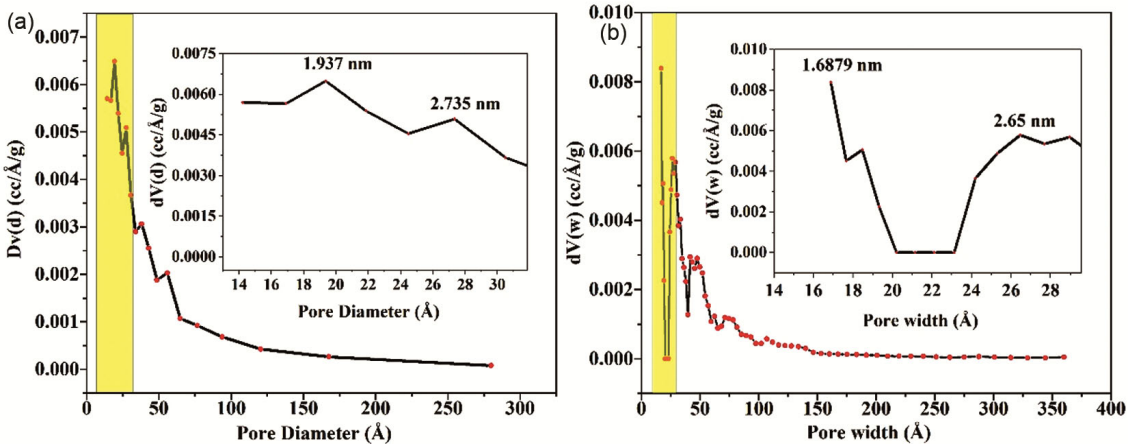

Fig. 7 — Pore size distribution obtained by (a) BJH method and (b) DFT method

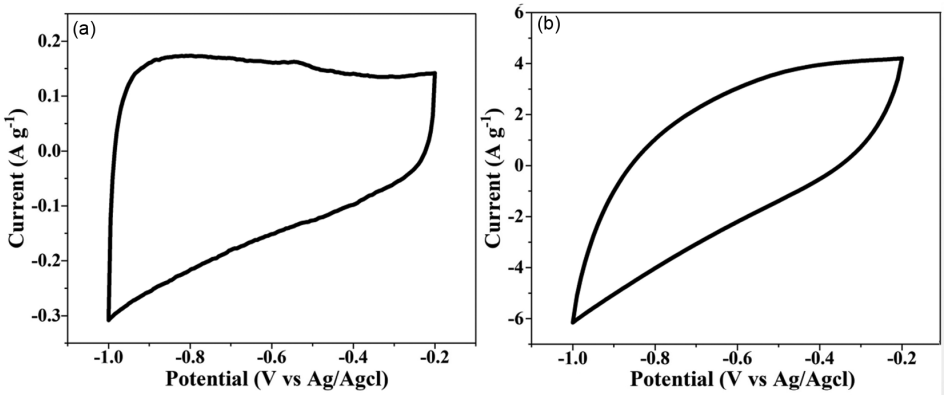

Fig. 8 — CV of lampblack electrode at (a) 2 mVs^{-1} and (b) 100 mVs^{-1}

3.2 Electrochemical Measurements

Figure 8 shows the Cyclic Voltammetry (CV) profiles of lampblack-based electrode scanned between -1 V to -0.2 V. Fig. 8(a) is the CV recorded at scan rate of 2 mVs^{-1} and Fig. 8(b) is the CV recorded at 100 mVs^{-1}. At a low scan rate of 2 mVs^{-1}, the CV curves demonstrate quasi-rectangular shape. Generally, the CV curve of a pure carbon electrode displays a characteristic typical rectangular shape which indicates a pure capacitive behavior with no faradaic reactions[12]. The quasi-rectangular shaped curve in Fig. 8(a) shows the presence of both double layer capacitance and pseudocapacitance due to presence of functional groups in the carbon sample[9,33]. At high scan rate of 100 mVs^{-1}, the CV curve is tilted, however, it is still rectangular-like in shape[13].

Figure 9(a) shows the CV curves of the lampblack electrode at different scan rates from 2 mVs^{-1} to 100 mVs^{-1}. The specific capacitance corresponding to each scan rate was calculated using the following equation[34].

$$C_{sp} = \frac{A}{2km\Delta V} \quad \ldots(1)$$

where A is integrated area under curve, k is scan rate (mVs^{-1}), ΔV is potential window (V) and m is active mass (g) of material in the electrode.

Using the Eq. (1), the specific capacitance at scan rates of 2, 5, 10, 20, 50 and 100 mVs^{-1} are 74.87, 66.25, 57.51, 47.03, 31.76 and 21.11 Fg^{-1}, respectively. The result clearly shows that the value of specific capacitance is decreased as the scan rate is

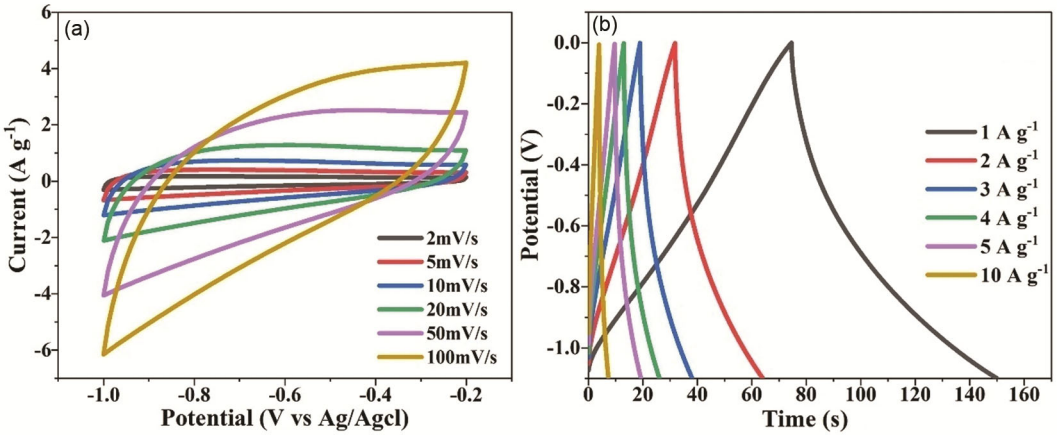

Fig. 9 — (a) CV cruves at different scan rates and (b) GCD curves at different current density

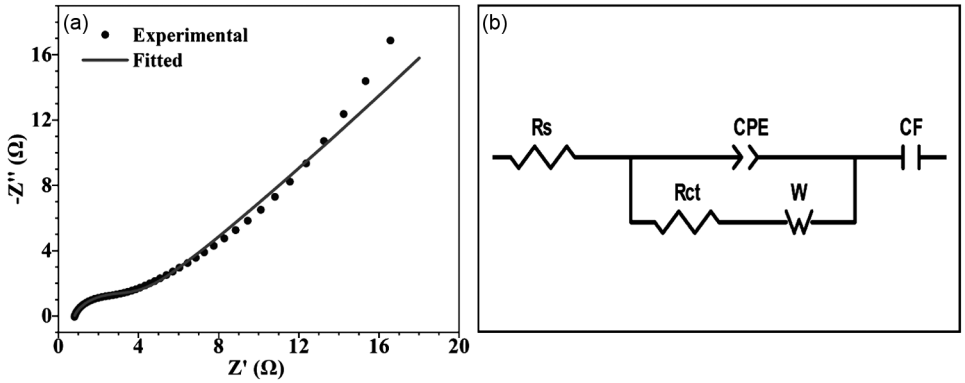

Fig. 10 — EIS spectrum of lampblack electrode a) Nyquist plot and b) equivalent circuit used to fit the Nyquist plot. Modified from ref.[38].

increased. This characteristic result indicates the presence of micropores in the lampblack[35].

To further investigate the electrochemical properties of the electrode, galvanostatic charge–discharge (GCD) tests were also performed. Fig. 9(b) shows the GCD curves at different current densityof 1, 2, 3, 4, 5 and 10Ag^{-1}. The corresponding specific capacitance obtained were 70.36, 60.61, 55.04, 51.83, 47.89 and 35.94 Fg^{-1}, respectively. The specific capacitance from the GCD test was calculated using the following equation[36].

$$C_{sp} = \frac{I\Delta t}{m\Delta V} \quad \ldots(2)$$

where I is the discharge current (A), Δt is the discharge time (s), ΔV is the potential window (V) and m is the active mass (g) of the material in the electrode.

The values of specific capacitance obtained from GCD test also show attenuation as the current density increases. This can be explained that at low current density, the ions of the electrolyte can easily enter the micropores and form a double layer. At high current density, the ions need to access the electrode surface as fast as possible but can only access the limited micropores. So, the double layer formation is decreased and hence the reduction in specific capacitance[8,9,12,33].However, due to the presence of pores from microporosity to mesoporosity in the lampblack, the bigger mesopores provide pathway to access smaller micropores[5,32]. So, the attenuation of the specific capacitance is not high when current density is increased. This shows the capacitive performance of olive oil lampblack-based electrode is satisfactory even at high current density. The GCD curves in Fig. 9(b) also shows slightly distorted from perfect triangular shape indicating existence of pseudocapacitance along with the formation of double layer capacitance in the electrode-electrolyte interface[24,37]. The GCD curves show negligible IR drop which indicates the excellent stability and reversibility of lampblack carbon[34].

Figure 10(a) represents the Nyquist plot of the lampblack electrode in which the horizontal and

vertical axes are real and imaginary components of the impedance, respectively. The Nyquist plot comprises a distored semi-circle in high frequency region and an imperfect linear part in low frequency region. The semi-circular in the Nyquist plot arises because of a parallel combination of capacitor and resistance[5]. In the working electrode prepared with porous carbonaceous material, capacitance can be attributed to existence of electrochemical double layered capacitance and pseudocapacitance[3,5,17]. On the other hand, the resistor is the interfacial resistance and the value of the resistor can be estimated by the diameter of the semicircle[5]. The semicircle is displaced along Z'axis due to existance of ohmic resistance in series with the parallel combination of the interfacial resistance and the capaciotor. The first intersection point of the semi-circle (in the high frequency region in the Nyquist plot) on the horizontal axis gives the value of the ohmic resistance which is often called equivalent series resistance (ESR)[27]. Fig. 10(b) is an equivalent circuit[38]used to fit the Nyquist curve. The R_s is equivalent series resistance (ESR). Similarly, R_{ct} is the charge transfer resistance at the electrode-electrolyte interface. The constant phase element (CPE) is used to represent the double layer capacitor at the electrode and electrolyte interface. Because of the imperfection of the semi-circle seen in the Nyquist plot(Fig. 10(a)), the double layered capacitor was replaced with CPE. C_F is the psedocapacitor[38].The shallow slope of the linear part in the Nyquist plot indicates the existence of the pseudocapacitance[5]. The pseudocapacitance can be due to the presence of functional groups in the lampblack[3,24,27]. The value of the ESR obtained from the curve fitting using the equivalent circuit was 0.81 Ω. The minimal IR drop seen in the GCD curves is attributed to low value of ESR. Generally, this ohmic resistance is mainly attributed to the sum of the intrinsic resistance of the material of electrode, the contact resistance between the current collector and the material of the electrode, and the solution resistance[39]. As the electrode was prepared solely with the lampblack without adding conducting enhancer like carbon black, hence, it can be understood that the contact resistance of the lampblack-current collector is low and the electric conductivity of the lampbalck is high. High concentration and interconnected structure of the carbon particles might have yielded higher conductivity of the olive lampblack based electrode. The low value of ESR enhances power-capability of supercapacitors[40]. This enhanced the high-rate capability of the supercapacitor electrode and justified the value of specific capacitance obtained from GCD curves at different current densities.

4 Conclusions

The lampblack of olive oil prepared with low-cost and facile method possessed relatively high surface area and hierarchal pores structures. The availability of both microporous and mesoporous pore structures along with the moderately high surface area of the lampblack carbon enhanced the fast transfer of ions into the deeper part of the electrode and helped in the formation of a double-layer in a much larger area enhancing the specific capacitance.Also, presence of oxygen functional groups introduced some pseudocapacitance in the electrode. The specific capacitance of the electrode obtained from the GCD test was 70.36 Fg^{-1} at the current density of 1 Ag^{-1} with a low Equivalent Series Resistance (ESR) value of 0.81 Ω. Good capacitive performance and low ESR value of the lampblack-basedelectrode indicate the potential use of olive oil lampblack for the preparation of low-cost and high-performance supercapacitor electrodes.

Acknowledgments

The authors acknowledge the support from PSC-CUNY grant, USA. Also, the authors are thankful to Prof. Nishith Verma and Dr. Rishabh Anand Omar (Project Scientist), Environmental Remediation Lab, Indian Institute of Technology (IIT), Kanpur, India, Prof. Sarang Ingalo, and Dr. Shiva Kant, department of MSE, IIT, Kanpur India, Associate Professor Sudarshana Shakya, Bhaktapur Multiple Campus (BMC), Tribhuvan University (T.U.), Dr. Tanka Mukhiya, Chemistry Department, BMC, T.U.,and Dr. Dibyashree Shrestha, Chemistry Department, Patan Multiple Campus, T.U., Nepal.

References

1 Becker H I, (to General Electric Company), *US Pat*, 2800616, (1957).
2 Conway B E, Birss V & Wojtowicz J, *J Power Sources*, 66 (1997) 1.
3 Kötz R & Carlen M, *Electrochimica Acta*, 45 (2000) 2483.
4 Frackowiak E & Béguin F, *Carbon*, 39 (2001) 937.
5 Ghosh A & Lee Y H, *Chem Sus Chem*, 5 (2012) 480.
6 Chen M, Kang X, Wumaier T, Dou J, Gao B, Han Y, Xu G, Liu Z & Zhang L, *J Solid State Electrochem*, 17 (2013) 1005.
7 Wang D, Geng Z, Li B & Zhang C, *Electrochimica Acta*, 173 (2015) 377.

8 Guo Y, Wang T, Chen X & Wu D, *J Power Sources*, 507 (2021) 230252.
9 He X, Lei J, Geng Y, Zhang X, Wu M & Zheng M, *J Phys Chem Sol*, 70 (2009) 738.
10 Wang G, Liang R, Liu L & Zhong B, *Electrochimica Acta*, 115 (2014) 183.
11 Mukhiya T, Dahal B, Ojha G P, Kang D, Kim T, Chae S-H, Muthurasu A & Kim H Y, *Chem Eng J*, 361 (2019) 1225.
12 Schütter C, Ramirez-Castro C, Oljaca M, Passerini S, Winter M & Balducci A, *J Electrochem Soc*, 162 (2014) A44.
13 Xiong W, Liu M, Gan L, Lv Y, Li Y, Yang L, Xu Z, Hao Z, Liu H & Chen L, *J Power Sources*, 196 (2011) 10461.
14 Singh G, Sharma M, Mathur A, Halder A & Vaish R, *J Electrochem Soc*, 168 (2021) 050551.
15 Kossyrev P, *J Power Sources*, 201 (2012) 347.
16 Petrov M, Lovchinov K, Slavov L, Stankulov T, Nichev H, Hikov T & Tyutyundzhiev N, *Physica Status Solidi (A)*, 218 (2021) 2000617.
17 Raj C J, Kim B C, Cho O-B, Cho W-J, Kim S-J, Park S Y & Yu K H, *Bull Mater Sci*, 39 (2016) 241.
18 Zhang B, Wang D, Yu B, Zhou F & Liu W, *RSC Adv*, 4 (2013) 2586.
19 Joshi P, Lawaju U & Binod B K, *BIBECHANA*, 17 (2020) 58.
20 Lawaju U & Joshi P, *J Nepal Phys Soc*, 8 (2022) 1.
21 Lawaju U, KC A & Joshi P, *Sci World*, 16 (2023) 94.
22 Joshi P, Lawaju U, KC A, Nakarmi M & Pradhan R, *BIBECHANA*, 20 (2023) 205.
23 Barbieri O, Hahn M, Herzog A & Kötz R, *Carbon*, 43 (2005) 1303.
24 Hor A A & Hashmi S A, *Electrochimica Acta*, 356 (2020) 136826.
25 Qu D & Shi H, *J Power Sources*, 74 (1998) 99.
26 Singh S, Bairagi P K & Verma N, *Electrochimica Acta*, 264 (2018) 119.
27 Shrestha L K, Shrestha R G, Maji S, Pokharel B P, Rajbhandari R, Shrestha R L, Pradhananga R R, Hill J P & Ariga K, *Nanomaterials*, 10 (2020) 728.
28 Kang D-S, Lee S-M, Lee S-H & Roh J-S, *Carbon Lett*, 27 (2018) 108.
29 KC A, Anderson J, Ayala A, Engdahl C, Piner E L & Holtz M W, *J Cryst Growth*, 610 (2023) 127172.
30 [Accessed September 16, 2023] Available from: https://www.sigmaaldrich.com/NP/en/technical-documents/technical-article/analytical-chemistry/photometry-and-reflectometry/ir-spectrum-table.
31 Sing K S W, *Pure Appl Chem*, 57 (1985) 603.
32 Shrestha L K, Shahi S, Gnawali C L, Adhikari M P, Rajbhandari R, Pokharel B P, Ma R, Shrestha R G & Ariga K, *Materials*, 15 (2022) 8335.
33 Karnan M, Subramani K, Srividhya P K & Sathish M, *Electrochimica Acta*, 228 (2017) 586.
34 34 Wang Y, Jiang L & Wang Y, *Electrochimica Acta*, 210 (2016) 190.
35 Xing W, Qiao S Z, Ding R G, Li F, Lu G Q, Yan Z F & Cheng H M, *Carbon*, 44 (2006) 216.
36 Shrestha D, Maensiri S, Wongpratat U, Lee S W & Nyachhyon A R, *J Environ Chem Eng*, 7 (2019) 103227.
37 Lawaju U, KC A & Joshi P, *Sci World*, 16 (2023) 94.
38 Subramani K, Sudhan N, Divya R & Sathish M, *RSC Adv*, 7 (2017) 6648.
39 Wang J-G, Yang Y, Huang Z-H & Kang F, *Carbon*, 61 (2013) 190.
40 Maletin Y, Strelko V, Stryzhakova N, Zelinsky S, Rozhenko A, Gromadsky D, Volkov V, Tychina S, Gozhenko O & Drobny D, *Energy Environ Res*, 3 (2013) 156.